communications biology

A Nature Portfolio journal

Article

https://doi.org/10.1038/s42003-025-08229-y

# An odorant receptor for a key odor constituent of ambergris



Dan Takase[1], Tomohiro Shirai[1], Kensuke Misawa[2], Hiroaki Matsunami[3] & Keiichi Yoshikawa[1]

Ambergris, a substance derived from the digestive system of sperm whales, has been valued for centuries for its unique aromatic properties. However, historical accounts indicate that certain human populations, particularly in East Asia, utilized ambergris without regard for its odor quality. These observations suggest that ambergris offers a model for studying how pleasant olfactory perception and its regional variations are constructed. Despite its historical and cultural significance, the molecular basis of ambergris perception has remained unclear. Here, we identified OR7A17 as an odorant receptor tuned to (-)-Ambroxide, a key odorant in ambergris. Analysis of genetic and functional variations in OR7A17 revealed that non-functional alleles of this receptor are prevalent in human populations, especially in East Asia. Individuals lacking functional *OR7A17* alleles could still detect (-)-Ambroxide but found its scent less pleasant compared to those with functional alleles. These findings elucidate a molecular mechanism that influences the perceived pleasantness of ambergris and shed light on its enduring legacy in perfumery.

Ambergris is a solid, waxy, flammable substance of a dull grey hue with a unique odor, rarely encountered as jetsam on beaches or within the carcasses of deceased sperm whales (*Physeter macrocephalus*). It originates from the digestive system of sperm whales, with references to its recognition dating back to at least the 13th century, as documented by Marco Polo[1,2]. As ambergris proceeds in the aging process, it undergoes a natural chemical transformation involving the oxidation of Ambrein, a primary and odorless constituent of ambergris (Fig. 1a)[3–5]. This transformation results in the production of (-)-Ambroxide, a key component that contributes to the unique and pleasant odor characteristic of ambergris.

The odor of ambergris / (-)-Ambroxide is characterized by various descriptors, including "amber", "woody", "green", "sweet", and "marine"[2,6]. It has been revered throughout history, with no suitable alternative found for other raw materials in perfumery. Jetsam ambergris has been traded at a premium price[1]. Historical figures, Queen Elizabeth I and Catherine de Medici, employed it to perfume their gloves[1,7]. Currently, chemically synthesized (-)-Ambroxides are widely employed as one of the most vital perfumery materials. Kaempfer noted in 1727 that the preferences for the scent of ambergris among East Asian ethnicities differ from those of Arabian ethnicities[8,9]. Specifically, the primary consumers of ambergris were Persians, Turks, and Arabs, who used it for perfuming. In contrast, East Asian ethnicities such as the Japanese and Chinese employed ambergris as a fixative to prolong the longevity of other fragrances, rather than emphasizing its odor quality. Therefore, ambergris may serve as a model for understanding how odor pleasantness is encoded in the olfactory system and how it varies depending on regions.

Humans have approximately 400 odorant receptor (OR) genes that constitute the largest group of G protein-coupled receptor genes[10,11]. These genes exhibit a significant enrichment of single nucleotide polymorphisms (SNPs) that modify OR function, resulting in an individually diverse array of functional ORs[12]. Each OR recognizes a unique subset of odorants on the olfactory sensory neurons scattered in the olfactory epithelium, while each odorant can be detected by multiple ORs with different sensitivity[13–16]. When exposed to a low concentration of an odorant, it is likely that ORs are not functionally redundant, and the most sensitive OR assumes a pivotal role in its detection[17–19]. Indeed, close to twenty ORs have been linked to the perceived sensitivity or intensity of specific odorants, based on their correlation with genetic and functional variation of an OR in individuals[20–29].

The activated ORs within the OE are then transmitted to various higher brain regions, encoding both the perception of a specific valence and the quality of the odor[30–32]. It is suggested that the valences of most odorants are not innate but acquired through learning[31]. Nonetheless, certain ORs likely exist as the genetic determinants for encoding valences[17,33–35]. By analyzing knockout mice, it has been proposed that the activation of a single OR elicits preference or aversive behavior, and the resulting behavior is determined by the summation of valences coded by the activated ORs[17]. However, there has been no instance of ORs in humans that are associated with the positive

[1]Sensory Science Research, Kao Corporation, 2606 Akabane, Ichikai-machi, Haga, Tochigi, 321-3497, Japan. [2]Biological Material Science Research, Kao Corporation, 2606 Akabane, Ichikai-machi, Haga, Tochigi, 321-3497, Japan. [3]Department of Molecular Genetics and Microbiology, Department of Neurobiology, Duke Institute for Brain Sciences, Duke University, Durham, NC, 27710, USA. e-mail: yoshikawa.keiichi@kao.com

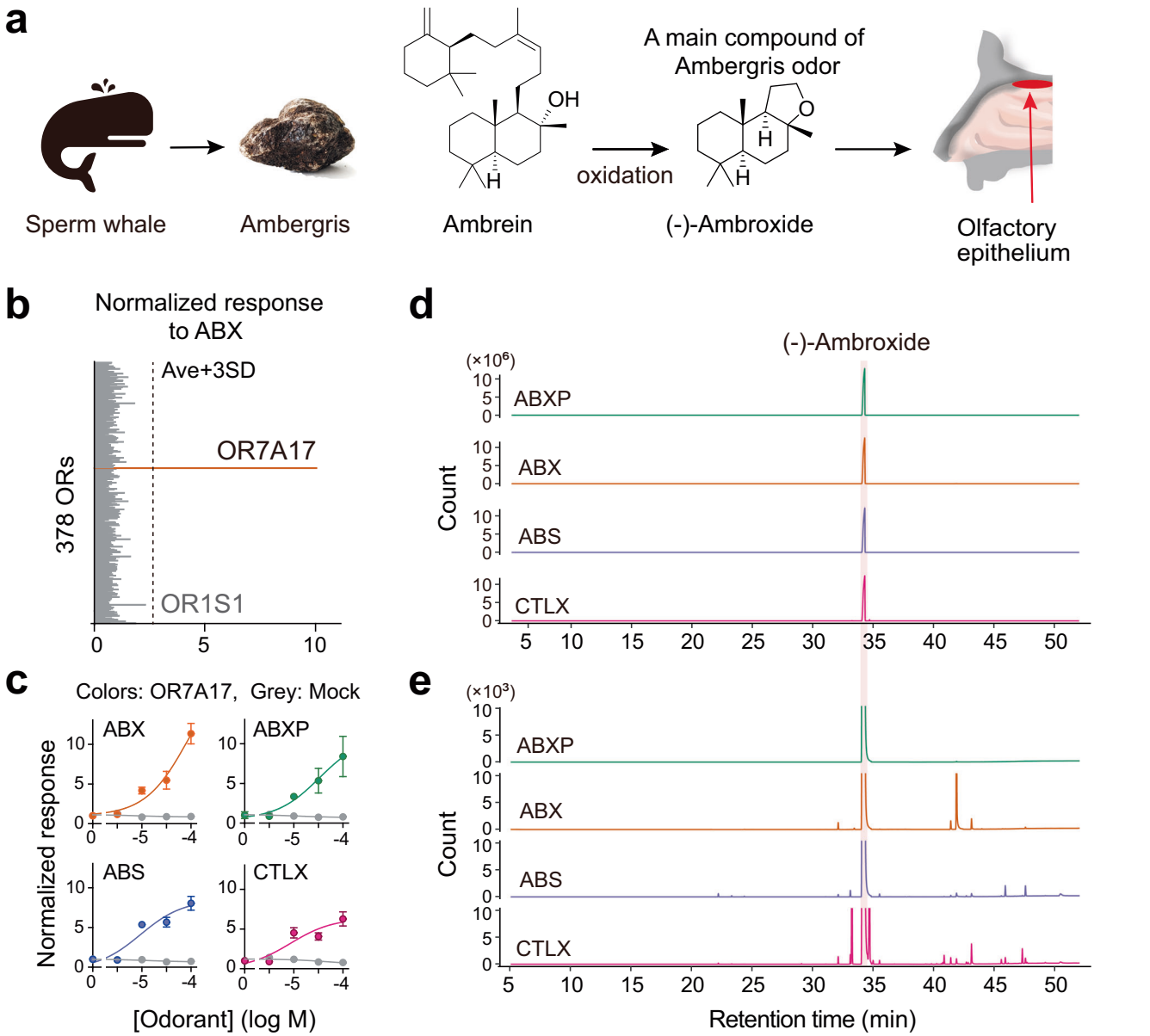


**Fig. 1 | Identification of a human odorant receptor for (-)-Ambroxide.** **a** Generation of a key odorant of ambergris. Ambergris is a solid substance produced as a metabolite of sperm whales. The major constituent of ambergris is Ambrein, which undergoes oxidative degradation, yielding (-)-Ambroxide as the key odor components of ambergris. **b** Screening of human ORs for (-)-Ambroxide. HEK293T cells expressing each of 378 ORs are stimulated with (-)-Ambroxide supplied as ABX (1.0 mM). Activation of each OR is shown as normalized response where a signal from ABX-stimulated cells was divided by that from non-stimulated cells expressing the same OR. The dashed line denotes mean augmented by three times the standard deviation (mean + 3 SD) of all the examined ORs. Data is mean values from two screening replicates. See also Supplementary Table 2 for statistics. **c** Dose-dependent response OR7A17 to three (-)-Ambroxides from different suppliers (ABX, ABS, and CTLX). ABXP denotes a purified sample of ABX. Data shown in black represents cells transfected without any ORs (mock). Data are shown as mean ± the standard error (SE) from three independent experiments. The normalized response is defined as the ratio of the mean luciferase signal in odorant-stimulated cells to that in non-stimulated cells. **d** GC/MS analysis of (-)-Ambroxide samples. The color lines represent total ion chromatogram. **e** An enlarged view of the y-axis depicted in Fig. 1d.

valence of an odorant with a mechanistic explanation, despite extensive efforts in large-scale studies focusing on nonfunctional genotypes of ORs, that is, natural knockout of ORs in individuals[21].

In this study, we investigated the human olfactory mechanism involved in eliciting the esteemed pleasant odor perception of a key odor constituent of ambergris. We conducted a screening of the majority of intact human ORs using a heterologous cell system. This screening identified an OR, that was narrowly tuned to (-)-Ambroxide. Further analysis revealed that the OR contains missense variants, leading to impaired receptor function. Exploiting the natural functional variants of the OR, a human study was conducted to test the associations between the functionality of the identified OR and the perception of (-)-Ambroxide. Our findings revealed a link between a specific OR and the perceived valence as well as the odor character of (-)-Ambroxide.

## Results

### Identification of an odorant receptor for (-)-Ambroxide

We conducted a screening of 378 ORs representing more than 95% of intact human OR genes. Each OR was expressed in HEK293T cells and stimulated with ABX, a commercially available (-)-Ambroxide. The activation of ORs was quantified using a luciferase reporter[36,37]. Subsequently, we identified OR7A17 based on the criterion that its response amplitude exceeded the mean + 3 standard deviations of all measured ORs (Fig. 1b). Although the second most robust response was observed from OR1S1, it did not meet the criterion. Furthermore, the responsiveness of OR1S1 was not reproducible in a subsequent dose-response analysis, whereas OR7A17 demonstrated a concentration-dependent response to ABX (Fig. 1c and Supplementary Figs. 1a).

In addition to ABX, OR7A17 was activated by two other (-)-Ambroxides, Ambrox Super (ABS) and CETALOX (CTLX, (±)-Ambroxide), supplied by different manufacturers (Fig. 1c). These consistent results suggest that the common and predominant compound, (-)-Ambroxide, is an agonist for OR7A17. However, these (-)-Ambroxides contain trace amounts of impurities (Figs. 1d, e). To rule out the possibility that the impurities were responsible for OR7A17 activation, we tested a purified sample of ABX with no detectable impurities (ABXP). The results showed that ABXP exhibited a comparable activity to ABX, ABS, and CTLX, indicating that OR7A17 is a receptor for (-)-Ambroxide (Fig. 1c).

OR7A17 has been reported to be expressed in the olfactory epithelium but has remained an orphan receptor[38]. The number of ORs activated by ABX appears to be smaller than those activated by other previously tested odorants in similar screening assays[13,37,39–42], although it should be interpreted with the caution due to potential failure of functional expression of ORs in vitro[43]. This outcome suggests that ABX is recognized through a small number of ORs, akin to other odorants such as musks, in which a single OR plays a significant role in its perception[18,22,26].

### Molecular receptive range of OR7A17

We hypothesized that OR7A17 commonly and selectively recognized odorants with an amber note and mediated the perceptual odor quality, analogous to the function of OR5A2 in musk compounds[23]. However, the molecular receptive range of OR7A17 was narrower than expected. OR7A17 displayed insensitivity to the majority of tested odorants with an amber note, as well as odorants with other odor characters (Figs. 2a, b, and Supplementary Figs. 1b-d)[6]. Only two structural analogues of ABX **1**, Orbitone (ORB) **2** and Iso E super (IES) **3**, activated OR7A17 (Figs. 2b, c). ORB **2** and IES **3** both contain the same compound as their primary constituent, albeit in varying isomeric proportions. To further elucidate the high selectivity, we investigated the structure-activity relationship. OR7A17 does not accept modifications of C-ring of (-)-Ambroxide, as evidenced by the substantially weaker activity of ORB **2**, Amberketal **6**, and Sclareolide **31** compared to ABX **1** (Figs. 2d, e). Given the unavailability of compounds with variations at the A-ring of (-)-Ambroxide, we chemically synthesized three derivatives via C-H halogenation of Sclareolide **31**, followed by subsequent derivatization (Fig. 2d, see **Methods** for synthetic routes)[44]. Two types of modification in the A-ring structure of (-)-Ambroxide (compounds **32** and **33**) significantly reduced the response of OR7A17, whereas epoxide **34** exhibited a similar response to (-)-Ambroxide (Fig. 2e). These findings highlight the limited tolerance of OR7A17 toward subtle structural variations of (-)-Ambroxide at both the C-ring and A-ring, realizing its highly selective tuning to (-)-Ambroxide. Thus, OR7A17 likely mediates the unique olfactory perception of (-)-Ambroxide /ambergris rather than general amber note.

### Human populations with genetic and functional variation of OR7A17

To dissect a role of a single OR in odor perception, natural functional variants of the ORs encoded in the human genome proves to be valuable. We searched for polymorphisms in a SNP database (1000 Genomes Project Phase 3) and identified two missense variants, rs10405129 and rs10404119 in *OR7A17* at frequencies greater than 1%. While these two polymorphisms did not exhibit a linkage disequilibrium with nearby ORs, they were found to be nearly completely linked to each other in this population (D': 1.0, $R^2$: 0.9937, Supplementary Fig. 2a, b). These polymorphisms lead to an allele with two amino acid changes (I46T and A69S), located in the first and second transmembrane domains, respectively (Fig. 3a). Hereafter, the most prevalent haplotype of *OR7A17* is denoted as IA, while the other is referred to as TS.

Our cell-based assay revealed an impaired function of OR7A17 TS. OR7A17 TS did not respond to ABX as well as other agonists for OR7A17 IA (Fig. 3b, Supplementary Fig. 1c and d). Both residues were found to be crucial for the function of OR7A17, as substitution of either amino acid resulted in diminished sensitivity to ABX. To gain insights into the substitution effects on OR7A17, we constructed a putative structure of OR7A17 using homology modeling and conducted a docking simulation. Given the two amino acids were apart from a predicted ABX-binding site (Fig. 3a), the loss of function of ORA17 TS could be attributable to its structural instability, which frequently impedes cell surface trafficking[43]. We measured cell-surface expression of OR7A17 IA and TS in HEK293T cells using flowcytometry via detecting their N-terminal FLAG tags. We observed moderate, yet significant decrease in the cell-surface expression levels of OR7A17 TS, suggesting that Ile46 and Ala69 play a role in structural stability of OR7A17 (Figs. 3c, d).

The global distribution of the *OR7A17* genotype was assessed using data from the 1000 Genomes Project Phase 3[45]. It revealed that the percentage of individuals homozygous for the insensitive allele (Thr46) varies from 0% (Luhya in Webuye, Kenya) to 50% (Southern Han Chinese, China) across different countries, with higher prevalence observed in East Asian populations, including the Japanese (22%, Fig. 3e). The frequency of the Ala69 variant in each region parallels that of the Ile46 variant, as the polymorphisms at amino acid positions 46 and 69 of *OR7A17* exhibit linkage disequilibrium (Supplementary Fig. 2b). These results identified a human population carrying the insensitive OR7A17, providing an opportunity to investigate its role in perception of (-)-Ambroxide.

### Humans perceive (-)-Ambroxide regardless of function of OR7A17

A human study was conducted to investigate a relationship between OR7A17 and the perception of (-)-Ambroxide. We sequenced *OR7A17* of 91 Japanese participants and revealed that 22 (24.2%) individuals were homozygous for the sensitive allele (IA/IA), 16 (17.6%) were homozygous for the insensitive allele (TS/TS), 52 (57.1%) were heterozygous (IA/TS), and one (1.1%) exhibited TS/TA. These frequencies align closely with the 1000 genome data mentioned earlier (Fig. 3e)[45]. Subsequently, 31 participants from all genotype category (ten for IA/IA, nine for IA/TS, and twelve for TS/TS) were recruited to engage in tasks aimed at evaluating perceptual sensitivity, pleasantness, and odor qualities.

Olfactory sensitivity of participants was assessed through multiple tasks. The first task measured detection threshold for ABXP using a three-alternative forced-choice procedure (Fig. 4a). Two participants who were unable to detect ABXP at maximum concentration (300 mM) were from TS/TS group. Although we observed a trend that TS/TS participants exhibited lower sensitivity to ABSP compared to IA/IA or IA/TS groups, it did not show statistical significance. To evaluate the impact of one functional allele, we combined participants possessing IA/IA and IA/TS genotypes for comparison with those exhibiting TS/TS genotype. Again, we observed a trend that TS/TS participants exhibited lower sensitivity to ABSP compared to IA/IA or IA/TS groups, but it was not statistically significant (Fig. 4b and Supplementary Data 1).

Prior studies reported associations between an OR genotype and olfactory sensitivity to an odorant using indices for the perceived intensity of the odorant, instead of measuring detection threshold (Fig. 4c)[20–22,25,26,33]. We therefore employed the previously published methodology with a seven-point scale of perceived odor intensity[26,33] and assessed 24 samples comprising four (-)-Ambroxides (ABXP, ABX, ABS, and CTLX), 19 odorants

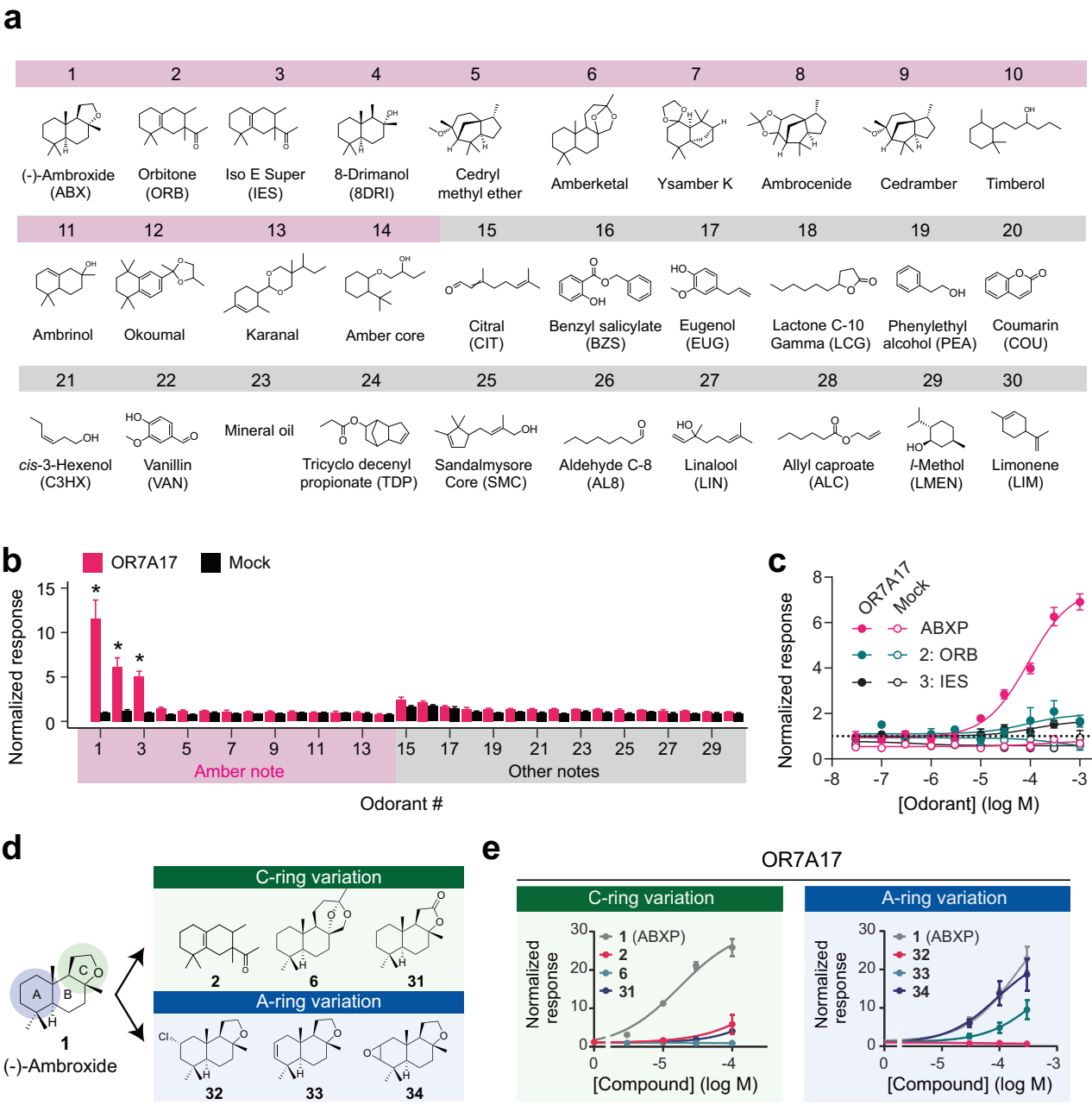


**Fig. 2 | Molecular receptive range of OR7A17. a** Chemical structures and names of tested odorants (#1-30), which are classified into odorants with or without amber note. Mineral oil is tested as solvent used in psychophysical tests. The abbreviations in parentheses are used in this manuscript. **b** Normalized response of HEK293T cells expressing OR7A17 against the odorants (100 μM). Black bars represent normalized response of mock-transfected cells. Odor quality of each odorant is referred from the public database[6]. Data is shown as mean ± SE from three independent experiments. Statistically significant deference in normalized response between OR7A17 and mock was determined using multiple *t*-test with the Sidak-Bonferroni method, with alpha = 5.0%. **c** Dose-dependent response OR7A17 to ORB **2** and IES **3**. The filled and white circles represent the data from OR7A17- and mock-transfected cells respectively. Data is shown as the normalized response (mean ± SE from three assay replicates of a representative experiment). **d** ABX analogs with varied substructures at A- or C-ring. Synthetic routes of the compounds are shown in Methods. **e** Dose-response analysis of OR7A17 to (-)-Ambroxides analogs. Data are shown as the normalized response (mean ± SE from three independent experiments).

with diverse odor quality, and a solvent. The activity of these samples for OR7A17 was shown in Fig. 2b. Neither ABXP nor the other three (-)-Ambroxides displayed significant differences in intensity perception (Figs. 4d, e, Supplementary Fig. 3a, and Supplementary Data 1). These results indicate that functional variation in OR7A17 does not account for individually different sensitivity to (-)-Ambroxide and almost all participants without functional OR7A17 were able to perceive odor emanating from (-)-Ambroxide. There likely exists other OR(s) that is unable to be functionally expressed in our heterologous cell system but contributes to olfactory sensitivity and odor intensity to (-)-Ambroxide. Although our results suggest a genotype-dependent difference in the intensity perception of Limonene (LIM), there is currently no mechanistic explanation, as OR7A17 TS was not sensitive to LIM in our in vitro assay system (Supplementary Fig. 1d).

## Pleasantness of (-)-Ambroxides is associated with function of OR7A17

Perceptual pleasantness of (-)-Ambroxides was evaluated using a visual analogue scale (Fig. 4c). Notably, among the 24 samples tested, the four (-)-Ambroxides were consistently ranked at the highest probability of

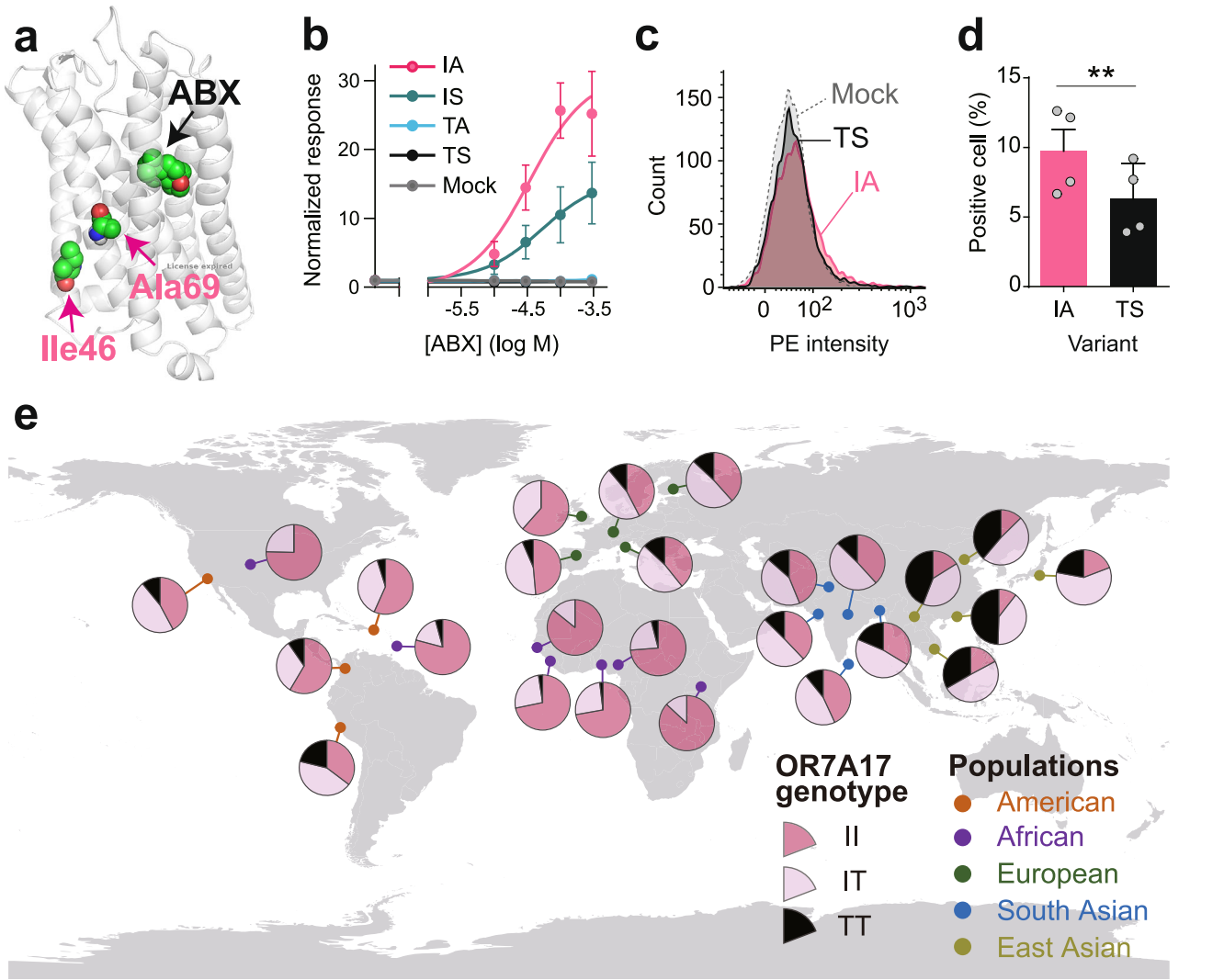


**Fig. 3 | Genetic and functional variation of OR7A17. a** The predictive binding pose of ABX with OR7A17. Carbon, oxygen, nitrogen, and hydrogen atoms are shown in lime green, red, blue, and white, respectively. Only the polar hydrogen atoms are shown. The structure was constructed based on consOR1 active state structure[57] using homology modeling. The docking simulation was performed using the AutoDock Vina program[61]. **b** ABX-sensitivity of OR7A17 with different pattern of substitutions at Ile46 and Ala69. Data is shown as the normalized response (mean ± SE from three independent experiments). **c** Cell-surface expression of OR7A17 with or without substitutions of I46T and A69S determined by flow cytometric analysis. Flag-Rho-tagged receptors were labeled with anti-Flag monoclonal antibodies and analyzed for surface expression. Phycoerythrin (PE)-conjugated antibody was used as a secondary antibody. The red and black histograms are a representative flow cytometric profile of OR7A17 with either IA or TS residues. The superimposed gray histograms show cells transfected without any exogenous receptors (Mock). **d** Summary of quantification of the amounts of receptors expressed on the cell-surface by flow cytometric analysis. The positive cells (%) was calculated as follows: the number of cells with PE fluorescence intensities exceeding the mean + 2 SD of mock-transfected cells divided by the total number of cells in each transfection condition. Data is shown as mean ± SE from four independent experiments. Asterisks indicate significant differences (Paired *t*-test, $^{**}P = 0.0061$). **e** Worldwide distributions of polymorphisms at amino acid positions 46 of *OR7A17*. The pie charts show the frequency of the genotypes in each population. Data is from 1000 Genomes Project Phase 3.

difference between participants with and without a functional *OR7A17* allele (Fig. 4f and Supplementary Data 1). In contrast, weaker agonists for OR7A17 (i.e., ORB **2** and IES **3**, Fig. 1c), along with other non-agonistic odorants, did not exhibit any *OR7A17* genotype-dependent differences. This is consistent with the interpretation from previous studies that the perception of odorants that only weakly activate a receptor will not be altered by functional variation in the receptor[20,26]. Participants with functional *OR7A17* recognized pleasantness when smelling each of the four (-)-Ambroxides including ABXP (Fig. 4g and Supplementary Fig. 3b). In contrast, participants lacking functional *OR7A17* answered significantly lower levels of pleasantness to ABXP. *OR7A17* genotype accounted for 14.7% of the variance in the pleasantness ratings of ABXP in our Japanese participants, as determined by multiple linear regression analysis, while sex and age accounted for 3.1% and 0.4%, respectively. This value of 14.7% is comparable to the contributions of single OR genotype to perceptual variations observed in a previous study[21]. The remaining variance may be attributable to another OR, environmental, or cultural factors not addressed in this study. It was possible that the lower pleasant perception was merely due to lower olfactory sensitivity to (-)-Ambroxide. Indeed, two participants who rated perceptual intensity of ABXP as zero answered no pleasantness. However, we did not observe a correlation between perceived pleasantness and olfactory sensitivity ($R^2 = 0.02$, Supplementary Fig. 3c). These findings provide evidence that OR7A17 is associated with pleasantness perception when smelling (-)-Ambroxide.

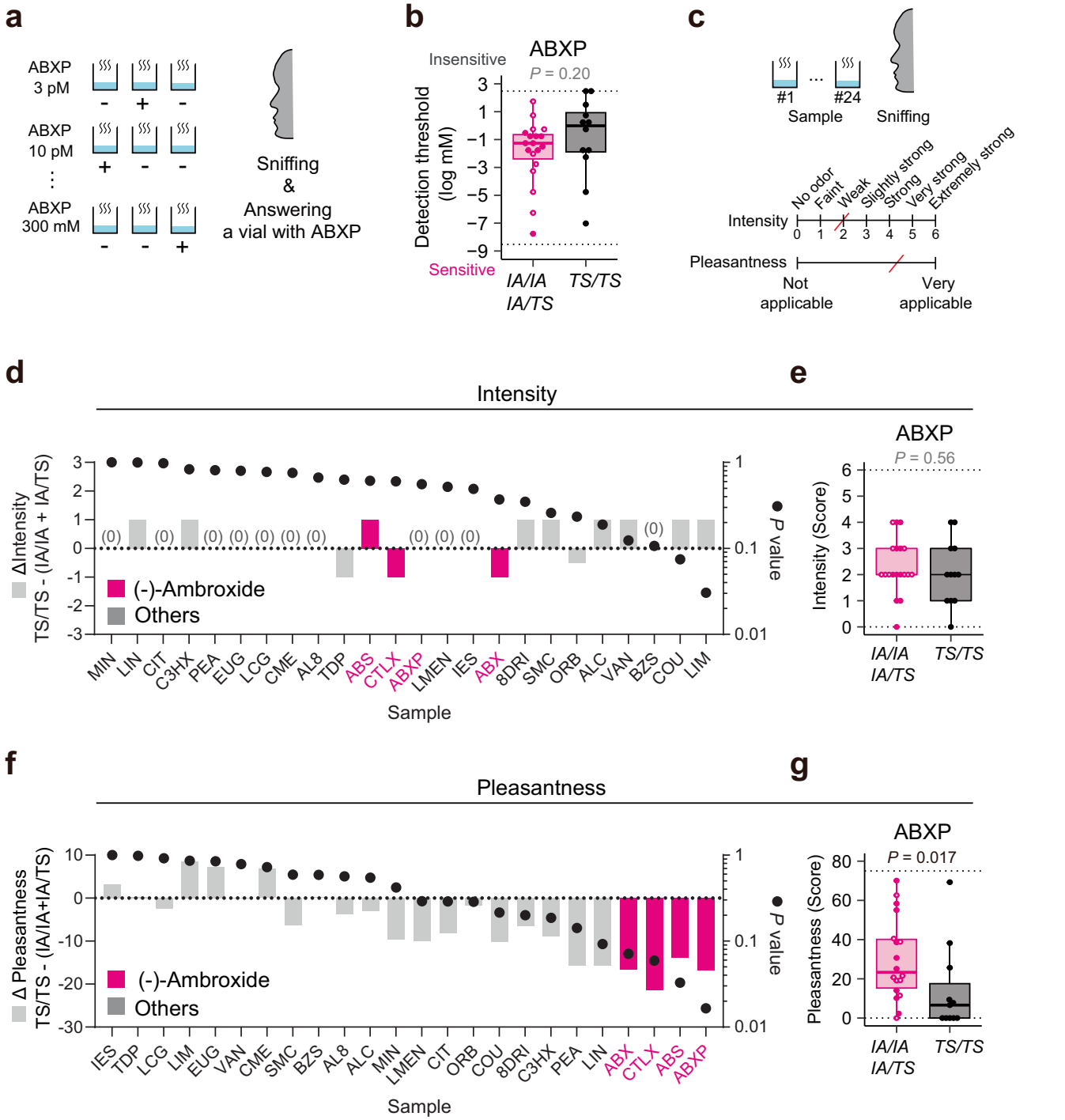


**Fig. 4 | OR7A17 variation affects pleasantness but not sensitivity to (-)-Ambroxide. a** Schematic drawing of method for measuring olfactory threshold. Thresholds were measured using a three-alternative forced-choice procedure. The participants were presented with three vials: one vial with a concentration of ABXP and the other two vial without ABXP. They sniffed and answered the ABX-containing vial. The trial began the lowest concentration of ABXP (3 pM). Incorrect answer led to the trail with next-higher concentration of ABXP. See Methods for details. **b** Detection threshold for ABXP. Each dot represents a minimum detectable concentration of ABXP of each participant. Participants are classified into two groups with at least one functional allele of *OR7A17* (IA/IA and IA/TS, $n = 19$) or not (TS/TS, $n = 12$). Heterozygous participants (IA/TS) were shown in open circles. The whisker plots show the median concentration, the first and third quartile and the upper and lower limits with Tukey's definition of outliers. **c** Method for measuring perceptual intensity and pleasantness of 24 samples. The participants sniffed 24 odors in a random order and evaluated their perceptual intensity and pleasantness separately. **d** Bars indicate differences in median of perceptual intensity of 24 odorant samples including solvent (mineral oil) between groups with or without at least one functional allele of *OR7A17*. For instance, the median perceived odor intensity values for the 19 participants with IA/IA or IA/TS genotypes and those with the TS/TS genotype both equate to two (Fig. 4e), resulting in a zero difference between the two groups. Dots show *P*-values that represent statistically significant difference in intensity perception of each odorant between the two groups. **e** Distribution of perceived intensity of ABXP measured in the two groups of participants. *P*-values are shown in Fig. 4d. **f** Differences in median of perceived pleasantness of 24 samples and their statistical significance. **g** Distribution of perceived pleasantness of ABXP measured in the two groups of participants. Statistical significance is assessed in B, D-G by Mann-Whitney *U* test with a significance level of 0.05. The dotted lines in panels B, E, and G represent the maximum and minimum values of the visual analogue scale for each experiment.

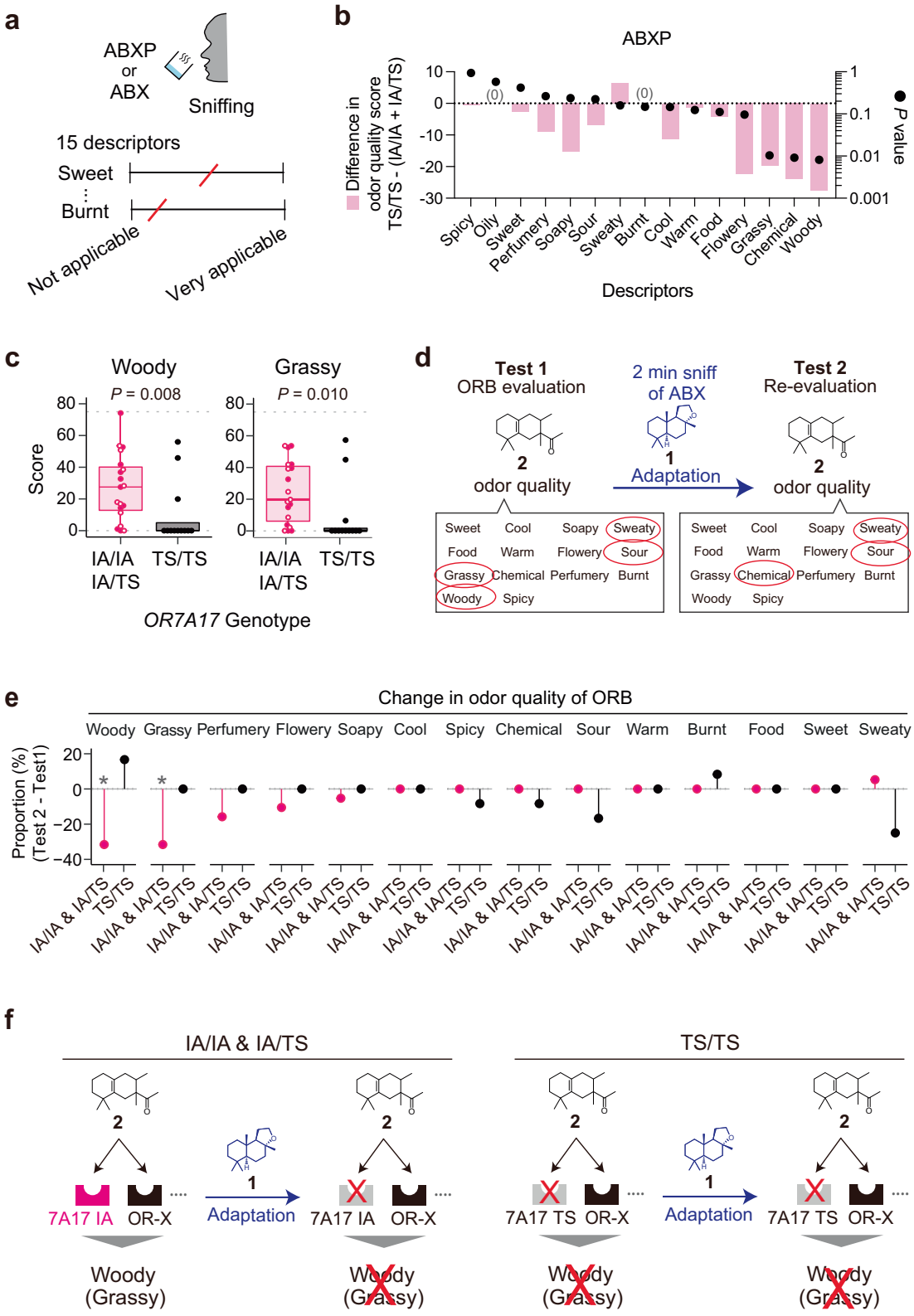


**Odor quality perception mediated by OR7A17**

The odor of (-)-Ambroxide/ambergris is described using a diverse array of descriptors including "amber", "woody", and "green"[2,6]. Here we asked whether OR7A17 is involved in evoking not only pleasantness but also distinct odor quality. In order to assess participants' perception of odor quality, we employed fifteen odor descriptors, incorporating some associated with (-)-Ambroxide/ambergris and others selected from prior reports (Fig. 5a)[2,6,46]. Certain descriptors related to Ambroxide/ambergris, such as "amber" were omitted due to potential unfamiliarity among untrained panels.

Untrained panels lacking functional *OR7A17* alleles answered lower scores when rating ABXP as "woody", a widely recognized descriptor of

**Fig. 5 | Perceived odor quality mediated by OR7A17. a** Schematic drawing of method for measuring perceived odor quality. The participants sniffed either ABX or ABXP and subsequently evaluated the applicability of each descriptor to their perceptions. **b***OR7A17* genotype-dependent perceived odor quality of ABXP. Bars indicate differences in median score of perceptual odor quality between groups with or without at least one functional allele of *OR7A17* (IA/IA and IA/TS, $n = 19$) or not (TS/TS, $n = 12$). Black dots show *P*-values that represent statistically significant difference in score of each odor quality descriptor between the two groups. **c** Distribution of woody and grassy odor descriptor scores of ABXP of participants. *P*-values are also shown in Fig. 5b. **d** An experimental design using intra-individual change in sensitivity of OR7A17. Perceived odor quality of ORB is evaluated by selecting corresponding descriptors before and after desensitization of ORs caused by 2 min smelling of ABX.**e***OR7A17* genotype-dependent difference in odor descriptor usage (%) for ORB between Test 1 and Test 2. The y-axis shows the subtraction of the odor descriptor usage in Test 1 from that in Test 2 (Test 2 – Test 1). $^*p < 0.05$, McNemar's test. Data shown are from 19 participants with *OR7A17 IA* and twelve participants with *OR7A17 TS/TS*. **f** A model for OR7A17-mediated odor quality perception based on the result of genotype-dependent effects of ABX adaptation.

(-)-Ambroxide (Figs. 5b, c, Supplementary Figs. 4a, b, and Supplementary Data 1)[6]. Similar trends were observed for notes of "chemical" and "grassy" (similar to "green") of ABXP. A consistent result was also obtained from ABX (Supplementary Figs. 4b and c). These results suggest that OR7A17 is required to elicit woody odor perception against (-)-Ambroxide. Our current set of descriptors did not enable us to pinpoint a distinct odor quality that participants lacking functional *OR7A17* alleles perceived more strongly than those with OR7A17.

To further test the role of OR7A17, we performed an additional experiment by taking advantage of intra-individual change in sensitivity of OR7A17. A prolonged exposure with a stronger agonist may induce higher level of desensitization of its receptors[47]. Thus, we applied a procedure of 2-min smelling of ABX, which is the strongest agonist for OR7A17 among tested odorants, to induce a desensitization of perceptual pathways of ABX including OR7A17 in participants (Fig. 5d). Following a 2-min exposure to ABX, eleven out of 18 participants with *OR7A17 IA* allele reported a diminished perception of the intensity of ABX, suggesting that they were in a state of desensitized ORs probably including OR7A17 (Supplementary Fig. 4d and Supplementary Data 1). In this condition, participants additionally rated three other woody odorants: ORB **2**, IES **3**, and Cedryl methyl ether (CME **5**, Fig. 2a). ORB **2** and IES **3** were weaker agonists for OR7A17 than ABX, whereas CME **5** had no activity to OR7A17. Remarkably, the participants perceived different odor quality with ORB **2** after the desensitization procedure, whereas participants lacking functional *OR7A17* allele did not (Supplementary Fig. 4e). The difference was attributed to a decrease in perceived odor quality of woody and grassy. Six out of seven participants who initially perceived ORB **2** as woody/grassy did not detect the woody odor quality after desensitization (Fig. 5e and Supplementary Fig. 4f). A similar trend was observed when they assessed IES **3** before and after 2-min smelling of ABX (Supplementary Fig. 4g). These changes in woody/grassy odor quality in perception of ORB **2** and IES **3** were probably dependent on OR7A17 because participants without a functional *OR7A17* allele did not show the changes (Fig. 5e). Our results indicate that OR7A17 participates in generating perception of pleasantness and woody/grassy odor quality with (-)-Ambroxide /ambergris (Fig. 5f).

## Discussion

The unique perceptual odor quality of (-)-Ambroxide /ambergris has attracted many perfumers and scientists throughout the ages. Generation of the perceived pleasantness of ambergris as well as its distinct odor quality entails multiple processes including activation of respective stages of neuronal substrates and its comparison with those in previous experiences. However, these all processes begin at the periphery, with the recognition of (-)-Ambroxide by ORs. In this study, we functionally identified OR7A17 for (-)-Ambroxide and human populations with high frequency of natural knockouts of *OR7A17*. The measured perceptions of the individuals indicate that the activity of OR7A17 is associated with the pleasantness of (-)-Ambroxide, implicating that OR7A17-mediated neural circuitry govern odor pleasant perception.

Our data suggests that (-)-Ambroxide is recognized through a small number of ORs. There are two potential limitations for this claim. It is possible that the heterologous cell-based assay system may not functionally express a significant portion of ORs[43]. Additionally, our OR library was constructed from a pool of genomic DNA from anonymous donors, which may represent a biased genotype of ORs within the human population. However, a previous large-scale analysis of mouse OSNs identified fewer OSN sensitive to (-)-Ambroxide[48]. Our result aligns with the understanding that odorants with fewer free rotatable bonds activate a smaller number of ORs[49,50]. The relatively low redundancy in sensing (-)-Ambroxide led to the finding that functional variability of a single OR is correlated with its perception. OR7A17 did not show a significant response to a structural analogue, Amberketal **6**. This partially explains a prior observation that impaired sensitivity to (-)-Ambroxide and Amberketal **6** in humans are not interrelated[51]. Consequently, we propose a strong association between (-)-Ambroxide and OR7A17 in olfaction. Smaller repertoire of receptors and narrowed receptive range are likely to confer the advantage of minimizing the risk of misinterpreting non-essential signals as crucial ones.

In this study, we exclusively examined Japanese participants, which could raise concerns about the generalizability of the identified association to populations in other countries. Additionally, the relatively small number of participants whose ORs other than *OR7A17* were not genotyped may introduce the possibility that individuals had a biased genotype of other ORs. However, it is less likely that a causal OR is other OR(s) closely located with *OR7A17* as the polymorphisms of *OR7A17* did not exhibit a linkage disequilibrium with nearby ORs based on data from the JPT (i.e., Japanese in Tokyo) in the 1000 Genome Project phase 3[52]. A prior study has demonstrated a consistent genotype-perception association in multiple cohorts from diverse countries[25]. We posit that the identified genotype-pleasantness association is robust, as indicated by the statistical significance that were obtained consistently from multiple (-)-Ambroxides despite the small number of non-trained participants. Thus, the present study offers a model pair of an odorant and an OR associated with individually different odor perception that could be reproduced with a small size of non-trained panels. Regarding detection thresholds, a future study involving a larger sample size of approximately 285 participants, as estimated by our power analysis, may be required to assess whether the observed trend of genotype-dependent differences is significant (Fig. 4b).

Our findings suggest that humans are capable of perceiving (-)-Ambroxide regardless of their genotype of *OR7A17*, likely due to the presence of other ORs. Consequently, individuals are likely to have opportunities to acquire learned preferences for (-)-Ambroxide through their experiences. Despite potential prior exposure to (-)-Ambroxide, individuals lacking a functional *OR7A17* allele indicated a lower perceived pleasantness of ABXP, suggesting that the pleasantness of (-)-Ambroxide/ambergris is not solely learned, but genetically influenced olfactory response mediated by OR7A17. ORs associated with positive valence have not been previously documented in humans, while close to twenty ORs have been associated with the perceived sensitivity or intensity of specific odorants[20–29]. In contrast, such receptors have been identified in other model animals and are dedicated to detecting chemosignals, including pheromones, which convey interspecies information[17]. What did OR7A17 evolve as a mean to sense? The answer to this question is not known. Nonetheless, an engineered human OR7A17 with 24 substations of amino acid residues conserved across mammalian orthologous (an evolutional consensus version of OR7A17; Supplementary Table 1)[23] exhibited a weak response to endogenous steroidal odorants, such as Androstenone, Androstadienone, and Estratetraenol (Supplementary Fig. 5). These odorants, which share structural similarities with (-)-Ambroxide, have been reported to exhibit

pheromone-like activities in mammals and primates[53,54]. We propose that OR7A17 has evolved to sense a bodily odorant derived from endogenous steroids in animals. Future studies utilizing functional assays of OR7A17 and its orthologs should aid in identifying a physiologically relevant ligand that explains the strong, yet enigmatic, attachment between humans and sperm whale ambergris, as well as shed light on an origin of odor pleasantness in humans.

The regional difference in frequency of *OR7A17* genotypes and the associated phenotype in this study suggests geography-dependent pleasant perception of (-)-Ambroxide. This geographic dependency appears to correspond to the historical significance of ambergris. Ancient literature documents the high regard for the odor of ambergris in Northern Africa, Europe, and the Middle East[8,9]. In contrast, the olfactory characteristics of ambergris were not valued in certain East Asian populations[8,9]. Consistently, East Asian populations exhibit a higher prevalence of non-functional *OR7A17* compared to other regions. This scenario is likely exceptional as a recent study demonstrated substantial global consistency in odor pleasant perception and there has been no example of ORs in humans that are associated with odor pleasantness[55]. However, the scenario could be possible by an exceptional molecular mechanism for sensing (-)-Ambroxide, which involves a smaller set of narrowly tuned ORs with geographical variation in functionality. The robust association between (-)-Ambroxide and OR7A17 linked to perceived pleasantness likely accounts for the perfumery history that ambergris / (-)-Ambroxide has been highly esteemed as a perfumery raw material without any suitable replacement by other compounds. Future research aimed at developing a more potent and selective agonist for OR7A17 could potentially contribute to a new chapter to the history.

## Methods

### Materials availability

All unique reagents generated in this study are available from the lead contact with a completed materials transfer agreement.

### Odorants

Sources of odorants used in this study are shown in Supplementary Table 3. Components of odorant mixture in the experiment shown in Supplementary Fig. 1c were reported previously in ref. 23. Each of the other odorants were prepared and stocked as 100 mM EtOH solution. These stock solutions were stored in a freezer and diluted with Dulbecco's Modified Eagle Medium (DMEM, 4.5 g/L glucose) for stimulation.

### General methods for synthesis

The chemical reaction equations are provided in Supplementary information. All reactions sensitive to air and/or moisture were carried out in oven-dried (>100 °C) glassware under argon or nitrogen atmosphere, and under anhydrous conditions otherwise noted. Anhydrous benzene, dichloromethane ($CH_2Cl_2$), *N*,*N*-dimethylformamide (DMF), and tetrahydrofuran (THF) were purchased from Kanto Chemical Co. Inc and used without further drying. All other reagents and solvents were purchased at highest commercial grade and used as supplied unless otherwise noted. Analytical thin-layer chromatography (TLC) was performed using E. Merck silica gel 60 F254 plates. Column chromatography was performed using YAMAZEN silica gel Universal Columns. $^1$H and $^{13}$C NMR spectra were recorded on a Bruker Avance-600 spectrometer with DCH cryoprobe and calibrated with residual undeuterated solvent as an internal reference [1H NMR, $CHCl_3$ (7.24); $^{13}$C NMR, $CDCl_3$ (77.0)]. Chemical shifts are reported in δ (ppm). Coupling constants are reported in Hz (hertz). The following abbreviations are used to designate the multiplicities: s = singlet, d = doublet, t = triplet, br = broad, m = multiplet.

### Synthetic procedures

**2-Chloro-sclareolide 35**. The synthesis of 2-Chloro-sclareolide **35** from (+)-Sclareolide **31** via C-H chlorination, as well as the preparation of the *N*-chloroamide used in this reaction, were carried out according to the procedures described in reference 1. Briefly, (+)-Sclareolide **31** (106 mg, 0.422 mmol) and $Cs_2CO_3$ (137 mg, 0.422 mmol) were added to a flask and dried under reduced pressure. *N*-Chloroamide (308 mg, 0.886 mmol) in dry benzene (1 mL) was added to the flask under Ar and dark condition, and the mixture was heated to 55 °C. The mixture was irradiated by two CFL bulbs (Panasonic® Palook ball, EFD25EL/20E/2 T), and covered by aluminum foil. After being stirred at 55 °C for 24 h, the mixture was diluted with EtOAc, filtered, and concentrated under reduced pressure. The residue was subjected to column chromatography on silica gel (15 to 40% EtOAc/hexane) to afford 2-Chloro-sclareolide (71.1 mg, 59%) as a colorless oil: $^1$H NMR (600 MHz, $CDCl_3$) δ 4.20 (tt, *J* = 12.2, 4.2 Hz, 1H), 2.41 (dd, *J* = 16.2, 14.8 Hz, 1H), 2.25 (dd, *J* = 16.2, 6.5 Hz, 1H), 2.08 (dt, *J* = 12.0, 3.3 Hz, 1H), 2.03-1.95 (m, 3H), 1.88 (m, 1H), 1.68 (td, *J* = 12.2, 4.2 Hz, 1H), 1.51 (t, *J* = 12.7 Hz, 1H), 1.40-1.31 (m, 2H), 1.31 (s, 3H), 1.11 (dd, *J* = 12.7, 2.7 Hz, 1H), 0.95 (s, 3H), 0.94 (s, 3H), 0.87 (s, 3H); $^{13}$C NMR (150 MHz, $CDCl_3$) δ 176.0, 85.8, 58.6, 55.7, 53.8, 52.4, 49.7, 38.4, 38.2, 35.8, 32.9, 28.6, 21.6, 21.3, 20.1, 15.8. These chemical shift values were identical to those reported previously[44]. Therefore, the stereochemistry of the introduced Cl is consistent with that described in the previous study[44].

**Diol 36**. To a suspension of $LiAlH_4$ (18.6 mg, 0.489 mmol) in THF (1.0 mL) was added **35** (63.3 mg, 0.222 mmol) in THF (1.2 mL) at 0 °C. After being stirred at room temperature for 2 h, the reaction was quenched with EtOAc. Small amount of water was added to the mixture, and the mixture was filtered. The filtrate was washed with brine, and the organic layer was dried over $Na_2SO_4$, filtered, and concentrated under reduced pressure. The residue was subjected to column chromatography on silica gel (loaded with $CHCl_3$, 60 to 100% EtOAc/hexane) to afford diol **36** (41.8 mg, 65%) as a white solid: $^1$H NMR (600 MHz, $CDCl_3$) δ 4.16 (tt, *J* = 12.2, 4.1 Hz, 1H), 3.79 (m, 1H), 3.47 (m, 1H), 2.94 (br, 2H), 2.18 (m, 1H), 1.95 (ddd, *J* = 12.8, 4.1, 2.1 Hz, 1H), 1.90 (dt, *J* = 12.5, 3.1 Hz, 1H), 1.70-1.59 (m, 3H), 1.50-1.43 (m, 2H), 1.33 (m, 1H), 1.27-1.20 (m, 2H), 1.16 (s, 3H), 0.98 (dd, *J* = 12.2, 2.1 Hz, 1H), 0.93 (s, 3H), 0.82 (s, 3H), 0.82 (s, 3H); $^{13}$C NMR (150 MHz, $CDCl_3$) δ 72.7, 63.7, 58.8, 55.2, 55.0, 52.0, 49.8, 43.8, 41.4, 35.9, 33.2, 27.8, 24.6, 21.9, 20.0, 15.9.

**2-Chloro-Ambroxan 32**. To a solution of diol **36** (85.9 mg, 0.297 mmol) in nitromethane (3 mL) was added *p*-toluenesulfonic acid (TsOH)-$H_2O$ (33.9 mg, 0.178 mmol). After being stirred at room temperature for 6 h, the mixture was diluted with $Et_2O$, and was washed with saturated $NaHCO_3$ aq. and brine. The organic layer was dried over $Na_2SO_4$, filtered, and concentrated under reduced pressure. The residue was subjected to column chromatography on silica gel (5 to 20% EtOAc/hexane) to afford 2-Chloro-ambroxan **32** (47.8 mg, 59%) as a white solid: $^1$H NMR (600 MHz, $CDCl_3$) δ 4.24 (tt, *J* = 12.1, 4.1 Hz, 1H), 3.91 (td, *J* = 8.9, 3.4 Hz, 1H), 3.82 (dd, *J* = 16.5, 8.2 Hz, 1H), 2.05 (ddd, *J* = 12.4, 4.1, 2.2 Hz, 1H), 1.98 (ddd, *J* = 12.7, 4.4, 2.2 Hz, 1H), 1.94 (dt, *J* = 11.9, 3.2 Hz, 1H), 1.79-1.69 (m, 3H), 1.50 (t, *J* = 12.7 Hz, 1H), 1.44 (dd, *J* = 12.7, 7.3 Hz, 1H), 1.42-1.32 (m, 1H), 1.27 (m, 1H), 1.06 (s, 3H), 1.00 (dd, *J* = 12.4, 2.7 Hz, 1H), 0.94 (s, 3H), 0.86 (s, 5H); $^{13}$C NMR (150 MHz, $CDCl_3$) δ 79.7, 64.9, 59.7, 56.3, 55.0, 52.6, 50.3, 39.4, 38.6, 35.9, 33.3, 22.5, 21.6, 21.2, 20.2, 15.7.

**2,3-Dehydro-ambroxide 33**. To a solution of **32** (27.9 mg, 0.103 mmol) in DMSO (1.03 mL) was added *t*BuOK (116 mg, 1.03 mmol). After being stirred at 80 °C for 20 h, the mixture was diluted with $Et_2O$ and saturated $NH_4Cl$ aq. The organic layer was separated and the aqueous layer was extracted with $Et_2O$. The combined organic layer was washed with brine, dried over $Na_2SO_4$, filtered, and concentrated under reduced pressure. The residue was subjected to column chromatography on silica gel (5 to 18% EtOAc/hexane) to afford 2,3-dehydro-ambroxide **33** (16.8 mg, 70%) as a white solid: $^1$H NMR (600 MHz, $CDCl_3$) δ 5.42 (ddd, *J* = 10.0, 5.4, 2.4 Hz, 1H), 5.37 (m, 1H), 3.91 (ddd, *J* = 8.2, 8.2, 3.1 Hz, 1H), 3.81 (td, *J* = 8.2, 8.2 Hz, 1H), 1.98-1.94 (m, 1H), 1.81-1.69 (m, 5H), 1.45-1.34 (m, 3H), 1.28-1.24 (m, 1H), 1.08 (s, 3H), 0.96 (s, 3H), 0.88 (s, 3H), 0.85 (s, 3H); $^{13}$C NMR (150 MHz, $CDCl_3$) δ 138.5, 121.2, 79.7, 64.9, 58.8, 52.8, 40.4,

39.1, 35.2, 34.5, 31.9, 22.7, 22.2, 21.5, 20.5, 15.2. These chemical shift values were identical to those reported previously[56].

**2,3-Epoxy-ambroxide 34**. To a solution of **33** (16.8 mg, 0.0717 mmol) in $Et_2O$ (0.72 mL) were added $NaHCO_3$ (6.6 mg, 0.0788 mmol) and *m*CPBA (77% purity, 17.7 mg, 0.0788 mmol) at 0 °C. After being stirred at room temperature for 4 days, the mixture was diluted with $Et_2O$ and brine. The organic layer was separated and the aqueous layer was extracted with $Et_2O$. The combined organic layer was washed with brine, dried over $Na_2SO_4$, filtered, and concentrated under reduced pressure. The residue was subjected to column chromatography on silica gel (7 to 30% EtOAc/hexane) to afford 2,3-epoxy-ambroxide **34** (8.4 mg, 47%, dr~95:5 calculated from $^1$H NMR) as a white solid: $^1$H NMR for major diastereomer (600 MHz, $CDCl_3$) δ 3.89 (m, 1H), 3.80 (m, 1H), 3.19 (dd, $J$ = 5.9, 3.8 Hz, 1H), 2.79 (d, $J$ = 3.8 Hz, 1H), 1.90 (m, 1H), 1.83 (dd, $J$ = 14.8, 6.2 Hz, 1H), 1.76-1.63 (m, 3H), 1.44 (d, $J$ = 14.8 Hz, 1H), 1.37-1.22 (m, 3H), 1.10 (s, 3H), 1.10-1.07 (m, 1H), 1.03 (s, 3H), 1.00 (s, 3H), 0.84 (d, $J$ = 1.0 Hz, 3H); $^{13}$C NMR for major diastereomer (150 MHz, $CDCl_3$) δ 79.5, 64.8, 61.9, 58.4, 52.4, 47.4, 39.9, 38.7, 35.1, 32.5, 28.3, 22.5, 21.6, 20.8, 20.1, 17.4.

**Expression vector**. The sequence information of human ORs used in this study was reported previously[37]. Genes coding human ORs were amplified from human genomic DNA. The identified SNPs that were different from the reference sequences were not modified. When we amplified an OR gene with unknown missense mutations, we modified the genes with mutations to reference sequences. The human RTP1S gene was amplified from human genomic DNA, and it was inserted into pME18S without any N-terminal epitope tag.

**Designing consensus ORs**. BLASTP searches were conducted using a reference amino acid sequence of OR7A17 as a query against proteins in the database of reference proteins. As a result of the searches, 242 ORs more than 74% amino acid identity was identified. Amino acid alignment using ClustalW allowed identification of consensus amino acid residues, which were conserved across more than 50% orthologous receptors at a given site. A consensus amino acid was inserted into a human OR when more than 60% orthologous ORs had an amino acid at the position. An amino acid was deleted from a human OR when more than 60% orthologous receptor did not have an amino acid at the corresponding position. The consensus amino acid sequences were translated into DNA sequences through codon optimization. The DNA sequence of each OR was synthesized by GenScript Japan and inserted into a pME18S vector to generate OR proteins fused with N-terminal epitope tags of eight amino acids of FLAG tag, followed by twenty N-terminal amino acids of bovine rhodopsin.

**Cell**. HEK293T cells were grown in DMEM supplemented with 10% fetal bovine serum (FBS). Cells were cultured on a 100 mm cell culture dish at 37 °C in a humidified atmosphere containing 5% $CO_2$. Cells were split every two to four days before reaching confluence. When passaging cells, all medium in the cell culture was removed, and cells were gently washed with PBS. Trypsin-EDTA (0.25%) was used to detach cells from the bottom of the dish. Equal volumes of DMEM with 10% FBS were applied to the dish immediately after the cells detached. The cells' suspension was transferred to a 15 ml polypropylene tube and centrifuged for 1 min at 200 *g* at room temperature. DMEM and trypsin-EDTA were aspirated, and the retained cell pellet at the bottom of the tube was resuspended with DMEM with 10%. The cell suspension was transferred to a 100 mm cell culture dish with 9 ml DMEM and 10% FBS.

**Flow cytometry analysis**. HEK293T cells were grown to confluency, resuspended, and seeded onto 35-mm cell culture dish or 6-well plate. The number of seeded cells were $3.6 \times 10^5$ in 2 ml DMEM with 10% FBS. The cells were cultured overnight before transfection. The DNA transfection mixture in 100 µl DMEM contained 3 µg of FLAG-Rho-tagged OR, 1 µg RTP1S, and 10 µl polyethylenimine Max (PEI-MAX, 0.1%, pH 7.5). For preparing cells without any receptors (mock-transfected cells), 3 µg of empty vector was transfected instead of a FLAG-Rho-tagged OR, respectively. After incubation at room temperature for 15 min, the DNA transfection mixture was transferred to the cell culture dish. After 24 h, the cells were detached and resuspended with 1 ml cell stripper and 1 ml PBS with 2% FBS on ice. The cells in 15 ml polypropylene tubes (AGC TECHNO GLASS, Shizuoka, Japan) were centrifuged for 3 min at 200 g at 4 °C. The cell pellet at the bottom of the tube was resuspended with 120 µl of 0.3 µg/ml primary antibody [Anti-DYKDDDDK, Mouse-Mono (2H8)] in PBS with 2% FBS and incubated for 60 min on ice. At the end of the incubation period, the cells were washed with 1 ml PBS and 2% FBS twice and stained with 100 µl of 50 µg/ml phycoerythrin (PE)-conjugated goat anti-mouse IgG H&L antibody in PBS with 2% FBS for 30 min on ice in the dark. Dead cells were stained with 0.5 µg/ml, and 7-Amino-actinomycin D was added. The cells were analyzed using BD FACSuit with gating allowing for single, spherical, viable cells, and the measured PE fluorescence intensities were analyzed and visualized. The percentage of positive cells was calculated as follows: the number of cells with PE fluorescence intensities exceeding the mean + 2 SD of mock-transfected cells divided by the total number of cells in each transfection condition. Statistical analyses were performed using paired *t*-test.

**Dual-glo luciferase assay**. The Dual-Glo Luciferase Assay was used to determine the activities of firefly and Renilla luciferase in HEK293T cells[37]. Transfection and luciferase assays were performed as previously described. Briefly, 75 ng of a FLAG-Rho-tagged OR pME18S, 30 ng of CRE/luc2PpGL4.29, 30 ng of pRL-CMV, and 30 ng of RTP1S pME18S were applied in 10 µl DMEM with 0.41 µl of PEI-MAX (0.1%, pH 7.5) for each well of a poly-D-lysine-coated 96-well plate (Corning, NY, USA). For testing cOR7A17, 7.5 ng of a FLAG-Rho-tagged OR pME18S, 3.0 ng of CRE/luc2PpGL4.29, 30 ng of pRL-CMV, and 30 ng of RTP1S pME18S were applied. After incubation for 15 min, 90 µl of cell suspension ($2 \times 105$ cells/cm$^2$ in DMEM with 10% FBS) were added to the 10 µl transfection solution, and the plate was incubated for 24 h. For testing OR7A17 in Figs. 2b and 2c, 50 ng of a FLAG-Rho-tagged OR pME18S, 10 ng of CRE/luc2PpGL4.29, 10 ng of pRL-CMV, and 10 ng of RTP1S pME18S were applied in 10 ml DMEM with 0.41 ml of PEI-MAX (0.1%, pH 7.5) for each well of a poly-D-lysine-coated 96-well plate. After incubation for 15 min, 90 µl of cell suspension ($3 \times 105$ cells/cm$^2$ in DMEM with 10% FBS) were added to the 10 µl transfection solution, and the plate was incubated for 48 h. For each well of poly-D lysine-coated 384-well plate (Corning, NY, USA), 29 ng of a FLAG-Rho-tagged OR pME18S, 22 ng of CRE/luc2PpGL4.29, 11 ng of pRL-CMV, and 12 ng of RTP1S were applied in 4.4 µl DMEM with 0.16 µl of 0.1% PEI-MAX (0.1%, pH 7.5). After incubation for 15 min, 40 µl of cell suspension ($2 \times 105$ cells/cm$^2$ in DMEM with 10% FBS) was added to 4.4 µl of the transfection solution, and the plate was incubated for 24 h. The 384-well plate assay was performed using the BiomekFX laboratory automation system (Beckman Coulter, Brea, CA, USA). After 24 h of transfection, the medium was removed, and the transfected cells were stimulated with an odorant solution diluted in the DMEM (75 µl and 40 µl per well for 96-well plate and 384-well plate, respectively). The 96- or 384-well plates were sealed and incubated at 37 °C for 3-4 h. The luciferase reporter gene activities were measured by Mithras LB940 (Berthold Technologies, Bad Wildbad, Germany) and by Ensight multimode plate reader (PerkinElmer, Waltham, MA, USA).

**Molecular modeling**. We used the BLAST to search the proteins similar to human OR7A17 with known 3D structures. We selected the human consensus olfactory receptor (consOR1) as a template of homology modeling in complex with L-menthol (PDB ID: 8UXY)[57] because of low E-value (4e-136), high identity (64%), and the highest total score (389).

The 3D structure of human OR7A17 was constructed based on the consOR1 structure using the SWISS-MODEL server[58]. The model was refined as pH 7.5 using the PDB2PQR program (version 3.4.1)[59]. We prepared the initial 3D structure of (-)-Ambroxide using the EmbedMultipleConfs module of RDKit[60]. We docked the ligand using the AutoDock Vina program[61] as blind docking. The box center was defined as the centroid of the protein model and the box size was set as 60, 50, and 70 Angstrom, respectively. Exhaustiveness was 64. The top pose was selected as binding pose and depicted by PyMOL.

**Participants in the human study**. The study protocols # T147-180620 and #T271a-200420 were approved by the ethical review board of Kao Corporation. All ethical regulations relevant to human research participants were followed. Participants for this study were recruited from employees of Kao Corporation, who were not involved in olfaction-related research. Exclusion criteria for participation were chronic diseases, infection, medication, hormone replacement therapy, olfactory disfunction, subjective symptoms related to sense of smell, nasal diseases, pregnancy, breastfeeding, subjectively sensitive to fragrances or perfumes, and age outside the range of 20 to 59 years. Genotypes of *OR7A17* of a total of 91 subjects were determined in the study to recruit 20 participants with *OR7A17 IA/IA*, 20 with *OR7A17 IA/TS*, and 17 *OR7A17 TS/TS*. These target numbers of participants were based on a previous study that suggested the need for more than ten participants for each genotype group to detect a statistically significant difference in odor perception[26]. All participants provided informed consent to participate and received financial compensation for their time and effort. The genotype of one participant failed to be determined. Consequently, nine with IA/IA, eleven with IA/TS, and twelve with TS/TS agreed and completed the sensory tests.

Olfactory psychophysics were conducted between January and June 2020. Participants were instructed to refrain from engaging in vigorous physical activity, excessive alcohol consumption, and consuming pungent foods such as garlic and green onion on the day preceding the sensory tests. On the day of the tests, they were instructed to abstain from using fragrances, deodorants, hair styling products, hand creams, and any other scented products. Thirty minutes prior to the sensory tests, participants were instructed to refrain from smoking, eating, or consuming any beverages other than water. The test administrators were blind to genotype information of the participants.

**OR7A17 genotyping**. Genomic DNA was extracted from saliva samples using the Oragene® Discover kit (DNA Genotek Inc, Canada). Open reading frame of *OR7A17* was amplified through PCR with primers upstream (5'-ATGGAACCAGAGAATGACACAGGGATTTCA-3') and downstream (5'-GGAATAAGCTCAAAGTGAAAAACTGTCTTC-3'). The PCR was done using KOD-Fx Neo (TOYOBO). Cycling protocol was: 94 °C, 2 min; 40 cycles of 98 °C, 10 s; 68 °C, 2 min; and then 68 °C, 3 min. The PCR products were then cleaned up using NucleoSpin Gel and PCR Clean-up (MACHEREY-NAGEL) and sequenced.

**Procedures for measuring detection threshold of ABXP**. Olfactory thresholds were assessed using diluted odorants with odorless mineral oil in a 3-alternative forced-choice procedure[62]. A total of 23 concentrations of ABXP, ranging from 3 pM to 100 mM and 300 mM on a logarithmic scale, were prepared in 1 ml of mineral oil solution within 6 ml glass vials. During the initial trial, participants were presented with three sets of vials in a random order: one vial contained 3pM ABXP, while the others contained only the solvent (mineral oil). After sequentially sniffing from each vial, subjects were required to identify the one with an odor, without the need for recognition or quality identification. An incorrect detection prompted the presentation of the concentration two levels higher. Three consecutive correct detections of a concentration (i) resulted in the presentation of the next-lower concentration. Upon two consecutive correct detections, the participants were presented with the next-lower concentration, at which point they provided an incorrect detection, thus leading to an evaluation of the next-higher concentration until a concentration (iii) containing ABXP was consecutively detected. Finally, participants retested the lower concentrations. Upon two consecutive correct detections, the next-lower concentration was presented to identify a concentration (iv) at which the participants provided an incorrect detection. The olfactory threshold was determined as the concentration of the geometric mean of the two dilution steps (iii-iv). Note that the olfactory threshold for 8-drimanol was also measured in this study; however, no genotype-dependence was observed.

**Procedures for assessing odor intensity, pleasantness, and quality perception**. Participants were tasked with assessing the intensity and pleasantness of 24 odor samples presented to them. The samples were administered in a randomized order in a single-blind manner. They also evaluated odor quality of ABX and ABXP. Odor intensity was assessed using a seven-point scale in the sensory evaluation test, while perceived pleasantness and odor qualities were evaluated utilizing a 7.5 cm visual analogue scale. No reference odorants for each odor descriptor during the test procedure were provided. The evaluation process utilized the answer sheet depicted in Supplementary Figs. 6a-d. The concentrations and volumes of the samples were determined through a preliminary evaluation by multiple panelists to elicit intensity perception ranging from moderate to strong, as detailed in Supplementary Table 3.

**Sensory test to evaluate odor quality of odorants after odor adaptation**. Concentrations and volumes of test samples are listed in Supplementary Table 3. Participants evaluated odor intensity and quality of ABX, IES, ORB, and CME before and after two min smelling of ABX. The answer sheets are shown in Supplementary Figs. 6e and f. Specifically, participants were asked to smell the four odorant samples and record their perceived intensity of the odor on a 10 cm visual analogue scale, marked from 'Odorless' to 'Extremely strong'. Difference in odor quality before and after two min smelling of ABX was assessed using six-points scale. Participants selected odor descriptors they perceived from the four odorant samples. They were then given ABX and asked to inhale for two minutes. The four odorant samples would then be presented again in a different vial and participants were asked again to rate their perceived intensity and quality of the odor.

### Statistics and reproducibility

An odorant-induced activity in Dual-Glo luciferase assay was calculated as normalized response (fold increase). The normalized response was calculated as Luc(N) divided by Luc(0), where Luc(N) was the luminescence intensity of firefly luciferase divided by the luminescence intensity of Renilla luciferase of a certain odorant-stimulated well, and Luc(0) was the luminescence intensity of firefly luciferase divided by the luminescence intensity of Renilla luciferase of a certain non-stimulated well. A mean value of the normalized response was derived from two to three assay replicates within a single experiment. In a dose-response analyses, two statistical criteria were applied: (i) 95% compatibility intervals (CIs) of top and bottom parameters don't overlap, (ii) the extra sum-of-squares test to examine that the odorant-response curve is different from the curve obtained from mock-transfected cells ($P < 0.05$). We confirmed that the $EC_{50}$ values calculated from the sigmoidal curves with the normalized response values did not differ by more than 1 log step from those with raw firefly luciferase values. Data analysis was performed using Microsoft Excel, and data were fitted to a sigmoidal curve using GraphPad Prism software (version 8.3.0).

Individual-level data pertaining to psychophysics is presented in Supplementary Data 1, which enables the replication of our statistical analyses. The statistically significant differences in detection thresholds, perceived odor intensity, pleasantness, and quality between the two genotype groups were evaluated using the Mann-Whitney U test, with a significance threshold set at 0.05. The genotype-dependent differences in odor descriptor usage (%) for ORB were assessed using McNemar's test, also with

a significance level of 0.05. Concerning the contribution of the OR7A17 genotype to pleasant perception, the association was analyzed using multiple linear regression to regress the haplotype count (0, 1, or 2) of OR7A17 against scores of pleasantness using the R statistical package. To calculate the contribution (r2) of OR7A17 genotype to pleasantness scores, the percentage of variance explained by a linear model in which a covariate of OR7A17 genotype was removed was compared to the full linear model with covariates of OR7A17 genotype, age, and gender.

### Reporting summary

Further information on research design is available in the Nature Portfolio Reporting Summary linked to this article.

## Data availability

All data and any additional information required to reanalyze the data reported in this paper will be shared upon request. Numerical source data for all psychophysics graphs in the manuscript can be found in supplementary data 1 file.

Received: 11 January 2025; Accepted: 14 May 2025;
Published online: 23 May 2025

## References

1. Rowland, S. J., Sutton, P. A. & Knowles, T. D. J. The age of ambergris. *Nat. Prod. Res* **33**, 3134–3142 (2019).
2. Clarke, R. The origin of ambergris. *Latin American J. Aquatic Mammals* **5**, 7–21 (2006).
3. Ohloff, G., Schulte-Elte, K. H. & Müller, B. L. Formation of Ambergris Odorants from Ambrein under Simulated Natural Conditions. *Helv. Chim. Acta* **60**, 919–2766 (1977).
4. Awano, K., Ishizaki, S., Takazawa, O. & Kitahara, T. Analysis of ambergris tincture. *Flavour Fragr. J.* **20**, 18–21 (2005).
5. Yamabe, Y. et al. Construction of an artificial system for ambrein biosynthesis and investigation of some biological activities of ambrein. *Sci. Rep.* **10**, 19643 (2020).
6. Available online: www.thegoodscentscompany.com/ (accessed 31 Jan 2022). The Good Scents Company. (2022).
7. Dugan, H. *The Ephemeral History of Perfume: Scent and Sense in Early Modern England*. *The Ephemeral History of Perfume: Scent and Sense in Early Modern England* (2011).
8. Kaempfer Engelbert. *The History of Japan*. (1727).
9. Kentaro Yamada. *A Study of the History of Perfumery and Spices in the Far East*. (Chuokouronbijyutsu, 1976).
10. Niimura, Y., Matsui, A. & Touhara, K. Extreme expansion of the olfactory receptor gene repertoire in African elephants and evolutionary dynamics of orthologous gene groups in 13 placental mammals. *Genome Res* **24**, 1485–1496 (2014).
11. Billesbølle, C. B. et al. Structural basis of odorant recognition by a human odorant receptor. *Nature* **615**, 742–749 (2023).
12. Olender, T. et al. Personal receptor repertoires: olfaction as a model. *BMC Genomics* **13**, 414 (2012).
13. Saito, H., Chi, Q., Zhuang, H., Matsunami, H. & Mainland, J. D. Odor coding by a mammalian receptor repertoire. *Sci. Signal* **2**, 9 (2009).
14. Jiang, Y. et al. Molecular profiling of activated olfactory neurons identifies odorant receptors for odors in vivo. *Nat. Neurosci.* **18**, 1446–1454 (2015).
15. Katada, S., Hirokawa, T., Oka, Y., Suwa, M. & Touhara, K. Structural basis for a broad but selective ligand spectrum of a mouse olfactory receptor: Mapping the odorant-binding site. *J. Neurosci.* **25**, 1806–1815 (2005).
16. Mainland, J. D., Li, Y. R., Zhou, T., Liu, W. L. & Matsunami, H. Human olfactory receptor responses to odorants. *Sci. Data* **2**, 150002 (2015).
17. Horio, N., Murata, K., Yoshikawa, K., Yoshihara, Y. & Touhara, K. Contribution of individual olfactory receptors to odor-induced attractive or aversive behavior in mice. *Nat. Commun.* **10**, 209 (2019).
18. Sato-Akuhara, N. et al. Ligand specificity and evolution of mammalian musk odor receptors: Effect of single receptor deletion on odor detection. *J. Neurosci.* **36**, 4482–4491 (2016).
19. Dewan, A. et al. Single olfactory receptors set odor detection thresholds. *Nat. Commun.* **9**, 2887 (2018).
20. Mainland, J. D. et al. The missense of smell: Functional variability in the human odorant receptor repertoire. *Nat. Neurosci.* **17**, 114–120 (2014).
21. Trimmer, C. et al. Genetic variation across the human olfactory receptor repertoire alters odor perception. *Proc. Natl Acad. Sci. USA* **116**, 9475–9480 (2019).
22. Sato-Akuhara, N. et al. Genetic variation in the human olfactory receptor OR5AN1 associates with the perception of musks. *Chem Senses* **48**, bjac037 (2023).
23. Yoshikawa, K., Deguchi, J., Hu, J., Lu, H. Y. & Matsunami, H. An odorant receptor that senses four classes of musk compounds. *Curr. Biol.* **32**, 5172–5179.e5 (2022).
24. Menashe, I. et al. Genetic elucidation of human hyperosmia to isovaleric acid. *PLoS Biol.* **5**, e284 (2007).
25. Li, B. et al. From musk to body odor: Decoding olfaction through genetic variation. *PLoS Genet* **18**, e1009564 (2022).
26. Keller, A., Zhuang, H., Chi, Q., Vosshall, L. B. & Matsunami, H. Genetic variation in a human odorant receptor alters odour perception. *Nature* **449**, 468–472 (2007).
27. Jaeger, S. R. et al. A mendelian trait for olfactory sensitivity affects odor experience and food selection. *Curr. Biol.* **23**, 1601–1605 (2013).
28. McRae, J. F. et al. Identification of regions associated with variation in sensitivity to food-related odors in the human genome. *Curr. Biol.* **23**, 1596–1600 (2013).
29. McRae, J. F. et al. Genetic variation in the odorant receptor OR2J3 is associated with the ability to detect the 'grassy' smelling odor, cis-3-hexen-1-ol. *Chem. Senses* **37**, 585–593 (2012).
30. Stettler, D. D. & Axel, R. Representations of Odor in the Piriform Cortex. *Neuron* **63**, 854–864 (2009).
31. Root, C. M., Denny, C. A., Hen, R. & Axel, R. The participation of cortical amygdala in innate, odour-driven behaviour. *Nature* **515**, 269–273 (2014).
32. Miyamichi, K. et al. Cortical representations of olfactory input by trans-synaptic tracing. *Nature* **472**, 191–196 (2011).
33. Gisladottir, R. S. et al. Sequence Variants in TAAR5 and Other Loci Affect Human Odor Perception and Naming. *Curr. Biol.* **30**, 4643–4653.e3 (2020).
34. Kobayakawa, K. et al. Innate versus learned odour processing in the mouse olfactory bulb. *Nature* **450**, 503–508 (2007).
35. Yabuki, Y. et al. Olfactory receptor for prostaglandin F2α mediates male fish courtship behavior. *Nat. Neurosci.* **19**, 897–904 (2016).
36. Zhuang, H. & Matsunami, H. Evaluating cell-surface expression and measuring activation of mammalian odorant receptors in heterologous cells. *Nat. Protoc.* **3**, 1402–1413 (2008).
37. Ieki, T., Yamanaka, Y. & Yoshikawa, K. Functional analysis of human olfactory receptors with a high basal activity using LNCaP cell line. *PLoS ONE* **17**, e0267356 (2022).
38. Olender, T. et al. The human olfactory transcriptome. *BMC Genomics* **17**, 619 (2016).
39. Saito, N. et al. Involvement of the olfactory system in the induction of anti-fatigue effects by odorants. *PLoS One* **13**, e0195263 (2018).
40. Shirai, T. et al. Functions of human olfactory mucus and age-dependent changes. *Sci. Rep.* **13**, 971 (2023).
41. Fukutani, Y. et al. Antagonistic interactions between odorants alter human odor perception. *Curr. Biol.* **33**, 2235–2245.e4 (2023).
42. Ijichi, C. et al. Metabolism of odorant molecules in human nasal/oral cavity affects the odorant perception. *Chem. Senses* **44**, 465–481 (2019).
43. Ikegami, K. et al. Structural instability and divergence from conserved residues underlie intracellular retention of mammalian odorant receptors. *Proc. Natl Acad. Sci. USA* **117**, 2957–2967 (2020).

44. Quinn, R. K. et al. Site-Selective Aliphatic C-H Chlorination Using N-Chloroamides Enables a Synthesis of Chlorolissoclimide. *J. Am. Chem. Soc.* **138**, 696–702 (2016).
45. Altshuler, D. L. et al. A map of human genome variation from population-scale sequencing. *Nature* **467**, 52–58 (2010).
46. Keller, A. & Vosshall, L. B. Olfactory perception of chemically diverse molecules. *BMC Neurosci.* **17**, 55 (2016).
47. Gainetdinov, R. R., Premont, R. T., Bohn, L. M., Lefkowitz, R. J. & Caron, M. G. Desensitization of G protein-coupled receptors and neuronal functions. *Annu. Rev. Neurosci.* **27**, 107–144 (2004).
48. Nara, K., Saraiva, L. R., Ye, X. & Buck, L. B. A large-scale analysis of odor coding in the olfactory epithelium. *J. Neurosci.* **31**, 9179–9191 (2011).
49. Kaluza, J. F. & Breer, H. Responsiveness of olfactory neurons to distinct aliphatic aldehydes. *J. Exp. Biol.* **203**, 927–933 (2000).
50. Amoore, J. E. Stereochemical theory of olfaction. *Nature* **199**, 912–913 (1963).
51. Triller, A. et al. Odorant - Receptor interactions and odor percept: A chemical perspective. *Chem. Biodivers.* **5**, 862–886 (2008).
52. Genomes Project, C. et al. A global reference for human genetic variation. *Nature* **526**, 68–74 (2015).
53. Melrose, D. R., Reed, H. C. & Patterson, R. L. Androgen steroids associated with boar odour as an aid to the detection of oestrus in pig artificial insemination. *Br. Vet. J.* **127**, 497–502 (1971).
54. Zhou, W. et al. Chemosensory communication of gender through two human steroids in a sexually dimorphic manner. *Curr. Biol.* **24**, 1091–1095 (2014).
55. Arshamian, A. et al. The perception of odor pleasantness is shared across cultures. *Curr. Biol.* **32**, 2061–2066.e3 (2022).
56. Zoretic, P. A., Fang, H. & Ribeiro, A. A. Synthesis of d,l-Norlabdane Oxide and Related Odorants: An Intramolecular Radical Approach. *J. Org. Chem.* **63**, 7213–7217 (1998).
57. de March, C. A. et al. Engineered odorant receptors illuminate the basis of odour discrimination. *Nature* **635**, 499–508 (2024).
58. Waterhouse, A. et al. SWISS-MODEL: Homology modelling of protein structures and complexes. *Nucleic Acids Res.* **46**, W296–W303 (2018).
59. Jurrus, E. et al. Improvements to the APBS biomolecular solvation software suite. *Protein Sci.* **27**, 112–128 (2018).
60. Riniker, S. & Landrum, G. A. Better Informed Distance Geometry: Using What We Know to Improve Conformation Generation. *J. Chem. Inf. Model* **55**, 2562–2574 (2015).
61. Eberhardt, J., Santos-Martins, D., Tillack, A. F. & Forli, S. AutoDock Vina 1.2.0: New Docking Methods, Expanded Force Field, and Python Bindings. *J. Chem. Inf. Model* **61**, 3891–3898 (2021).
62. Yoshikawa, K. et al. The human olfactory cleft mucus proteome and its age-related changes. *Sci. Rep.* **8**, (2018).


## Acknowledgements

The authors thank Hiroko Takatoku for conducting initial OR assays and a preliminary human study, Ryoichi Matsui for initial molecular modeling of OR7A17, Mari Kobayashi and Kaori Matsumoto for preparing plasmids and for supporting OR assays. This work was supported by grants from National Science Foundation grant 1555919 to H.M., National Institutes of Health grant DC014423 and DC016224 to H.M.

## Author contributions

D.T. designed, performed experiments, and wrote the manuscript. T.S. synthesized structural analogues of (-)-Ambroxide and wrote the manuscript. K.M. performed prediction of a structure of OR7A17. K.Y. conceived the project, designed experiments, performed experiments related to cell-surface expression of ORs and wrote the manuscript. H.M. wrote the manuscript.

## Competing interests

D.T., T.S., K.M., and K.Y. are employees of Kao Corporation. These do not alter the authors' adherence to all policies on of the journal sharing data and materials. Kao has applied for patents related to OR7A17. There are no products in development or marketed products to declare. H.M. has received royalties from ChemCom, research grants from Givaudan, and consultant fees from Kao Corporation.

## Additional information

**Supplementary information** The online version contains supplementary material available at https://doi.org/10.1038/s42003-025-08229-y.

**Correspondence** and requests for materials should be addressed to Keiichi Yoshikawa.

**Peer review information** *Communications Biology* thanks Luis Saraiva and the other, anonymous, reviewer(s) for their contribution to the peer review of this work. Primary Handling Editors: Joao Valente.